Journal of Solid Mechanics Vol. 12, No. 1 (2020) pp. 102-120
DOI: 10.22034/jsm.2019.584898.1395

Determination of the Effective Parameters for Perforated Functionally Graded Plates with Polygonal Cutout by Analytical Solution

M. Jafari [1,*], M.H. Bayati Chaleshtari [2], H. Abdolalian[1]

[1]*Faculty of Mechanical and Mechatronics Engineering, Shahrood University of Technology, Shahrood, Iran*
[2]*School of Mechanical Engineering, Iran University of Science and Technology, Narmak, Tehran, Iran*

Received 1 November 2019; accepted 4 January 2020

ABSTRACT

This paper investigates the moments and stress resultants from infinite FG laminates with different polygonal cutouts subject to uniaxial tensile load. The analytical solution used for the calculation of stress resultants and moments is the basis of the complex-variable method and conformal mapping function. The impact of various factors, namely cutout orientation angle, cutout aspect ratio as well as the cutout corner curve on stress distribution and moment resultants is studied. The effect of the aforementioned parameters around triangular, square, pentagonal and hexagonal cutout is analyzed. The mechanical characteristics of the graded plates are hypothesized to vary throughout the thickness exponentially. Finite element numerical solution is employed to examine the results of the present analytical solution. This comparison showed a favorable agreement level among the acquired analytical and numerical outcomes.

Keywords: Analytical solution; Complex-variable method; Functionally graded plate; Polygonal cutout; Stress resultants and moments.

1 INTRODUCTION

THE engineering structures, different types of cutouts are made to satisfy some service requirements. These cutouts result in strength degradation of the structure and may lead to failure. It is observed that many failures in aircraft structures have happened in fastened joints having high stress concentrations. In order to predict the behavior of the structure with such cutouts, it is essential to study the effect of cutout geometry and loading conditions on the stress and moment resultants distribution around the cutouts. In recent decades, engineers and designers have shown growing interest to use of functionally graded materials (FGMs), because the structural can be

*Corresponding author.
E-mail address: m_jafari821@shahroodut.ac.ir (M.Jafari).

improved by the applied of FGMs, in which thermal or mechanical properties gradually change over one of the primary dimensions. These materials can, therefore, have a significant impact on the strength of structural members under various loadings. In this paper, we investigate the impact of different parameters on the distribution of stress and moment resultants around a polygonal cutout in a functionally graded plate.

2 LITERATURE REVIEW

The first use of the complex-variable method for solving boundary value problems in two-dimensional elasticity for isotropic elastic materials is attributed to Muskhelishvili [1]. Savin [2] used this method to study infinite isotropic plates with different cutouts and anisotropic plates with elliptical and circular cutouts. Later, Muskhelishvili's method was expanded to two-dimensional problems of anisotropic elastic materials by Lekhnitskii [3]. The aim of Lekhnitskii when developing his theory was to provide a general solution for infinite anisotropic plates with circular cutouts of different sizes. But for simplicity's sake, he first developed a formulation for orthotropic plates. Sharma [4,5] also analyzed the stress concentration factor around different cutouts. Rezaeepazhand and Jafari [6] studied infinite plates with polygonal cutouts by the use of an analytical solution and examined the effect of parameters such as loading direction and cutout orientation.. Ukadgaonker and Rao [7] analyzed the stress in asymmetrically laminated plates with cutouts of different shapes, including circle and square as well as a number of irregular shapes. Bayati and Jafari [8] investigated the optimum design of isotropic finite plates with different polygonal cutouts under in-plane loading (uniaxial tensile, biaxial, and pure shear load). They used for the calculation of stress concentration is based on analytical solution of Muskhelishvili complex variable and conformal mapping with plane stress assumption. Moreover, Jafari and Bayati [9] relying on Lekhnitskii's analytical solution and expanding this solution to the polygonal cutouts in orthotropic plates, Comprehensive stress analysis of perforated orthotropic plates is conducted. In this research, design variables are load angle, bluntness, cutout orientation and fiber angle. In addition, using genetic algorithm Jafari et al. [10] obtained the optimal values of the parameters that affect the stress distribution around different cutouts in orthotropic and laminated composite plates. Chen et al. [11] investigated the stress distribution in a functionally graded plate (with varying properties along the radial direction) containing a circular cutout. Sharma [12] obtained stress functions for determining the stress distribution around special cutouts in infinite laminated plate subjected to arbitrary biaxial loading at infinity using Muskhelishvili's complex variable method. The effect of fiber orientation, stacking sequence, loading factor, loading angle and cutout geometry on stress distribution around cutouts in orthotropic/anisotropic plates was studied. Pan [13] provided an exact solution for functionally graded plate with circular cutout. Reid and Paskaramoorthy [14] employed the classical lamination theory to propose a solution for functionally graded plates. Uymaz and aydogdu [15] studied three-dimensional mechanical buckling of FG plates with general boundary conditions. Batra and Nie [16] used analytically plane strain static deformations of functionally graded eccentric and non-axisymmetrically loaded circular cylinders comprised of isotropic and incompressible linear elastic materials. Sharma and Dave [17] presented solution of stress resultant and moments around circular and elliptical cutout in infinite functionally graded plate with through-thickness material property variation. In this study, the complex-variable method was used to study the effect of parameters such as the distribution of material properties and loading angle on the stress resultants and moments. Chien et al. [18] investigated thermal buckling analysis is performed on hybrid functionally graded plates with an arbitrary initial stress. Joshi et al. [19] studied the effect of thermal environment on free vibration and buckling of partially cracked isotropic and FGM micro plates based on a non classical Kirchhoff's plate theory. Ashoori and Jafari [20] studied the effect of different parameters on stress resultant and moments distribution around non-circular cutouts in unsymmetrical laminates. They used complex potential approach ti examined the stress analysis of unsymmetrical laminates with non-circular cutouts. Jafari et al. [21] investigated optimum parameters involved in stress analysis of perforated plates, in order to achieve the least amount of stress around the square-shaped cutouts located in a finite isotropic plate using metaheuristic optimization algorithms. Moreover, Bayati and Jafari [22] studied the effective parameters involved in the stress analysis of perforated orthotropic plates, to achieve the lowest value of stress around the quasi-triangular cut-out located in an infinite orthotropic plate by using the Dragonfly Algorithm (DA) method. Sahu et al. [23] investigated the propagation of the surface wave in a piezo-structure. The structure consists of a LiNbO3 layer with flexoelectricity resting on PZT-5H half-space. Moreover, Sahu et al. [24] studied the transference of Love-type waves in functionally graded piezoelectric material layer bonded between viscous liquid and pre-stressed piezoelectric half-space. Following the elastic wave theory, the mathematical model was established. Wentzel–Kramers–Brillouin method was applied to obtain the theoretical derivations in functionally graded piezoelectric material stratum where variation in material gradients was taken exponentially.

Sahu et al. [25] presented study investigates the propagation of Love-type wave in functionally graded piezoelectric material (FGPM) layer bonded between piezomagnetic (PM) plate and pre-stressed piezoelectric (PE) half-space. Furthermore, Sahu et al. [26] studied of surface waves in functionally graded piezoelectric material (FGPM) clubbed between two dissimilar piezomagnetic (PM) media. The transference of elastic waves in a composite structure is analyzed following the elastic wave theory of magneto-electro-elasticity. Liouville-Green's (LG) approximation technique is used to solve the differential equation. The exponential variation is assumed in material gradients of FGPM stratum. Sahu et al. [27] used an analytical approach is adopted to investigate Rayleigh waves in a layered composite structure with corrugated boundaries. The structure of the model has been taken in such a way that the pre-stressed piezoelectric layer with rotation is lying over a pre-stressed, rotating, gravitational orthotropic substrate. Sahu et al. [28] presented model is considered to study the effect of material gradient coefficients and distinct parameters on Love-type surface wave propagation in FGPM layer bonded between pre-stressed piezoelectric layer and pre-stressed piezoelectric half-space. Sahu et al. [29] presented to compute the normal and shear stresses, dielectric, and electric potential in an irregular initially stressed piezoelectric substrate under moving load. A mathematical formulation of this physical problem gives rise to boundary value problem with the specified boundary conditions. In addition to, Sahu et al. [30] used an analytical approach is adopted to investigate the SH waves in a composite structure consisting of initially stressed rotating piezoelectric layer and initially stressed substrate with rotation. The interface between the layer and the substrate is assumed to be imperfect. Two distinct types of imperfect interfaces are considered.

The majority of previous studies on the functionally graded plates with cutouts has been focused on circular and elliptical shaped cutouts and has paid limited attention to parameters such as corner curvature and orientation angle of non-circular cutouts, despite their potentially major impacts on the strength of the structure. In this study, we investigate the effect of cutout orientation angle, aspect ratio, and cutout corner curvature on the stress distribution around polygonal cutout in functionally graded plates. The cutout is free of external loading and variation in mechanical properties of FGM is assumed to be exponential along the thickness. The plate is assumed to be extremely larger than its cutout (the plate is assumed to be infinite).

3 THEORETICAL AND NUMERICAL METHODS

In order to further develop Lekhnitskii's relation and to acquire stress resultants and moments dispersion at the proximity of the non-circular cutouts, as well as calculating Cauchy's integral in a simplistic manner amidst calculating the resultants, it is more favorable to turn the non-circular cutouts into a single circle. By utilizing a mapping function, the non-circular cutouts external area in the physical coordinate of z may be converted to the external area of the unit circle in plane ζ . The utilized mappings function in this evaluation [6]:

$$Z_{p_j} = \frac{1}{2}(a_j \zeta + \frac{b_j}{\zeta} + c_j \omega \zeta^n + (d_j \omega)/\zeta^n), \qquad j = 1,2,3,4 \tag{1}$$

Such that a_j ,b_j, c_j ,and d_j are:

$$\begin{aligned} a_j &= (1 - ics_j)\cos\beta + (-ic - s_j)\sin\beta \\ b_j &= (1 - ics_j)\cos\beta + (ic - s_j)\sin\beta \\ c_j &= (1 - is_j)\cos\beta + (i + s_j)\sin\beta \\ d_j &= (1 - is_j)\cos\beta + (-i - s_j)\sin\beta \end{aligned} \tag{2}$$

In the above equations, there are different parameters that various cutouts can be modeled by changing them, s_j are the roots of the characteristic equation of anisotropic plate, which will be described later; n shows the geometry of the cutout; in a way that n equal number of cutout sides minus 1. λ shows that how large is the cutout. For example, in above trigonometric equation, for quasi-square cutout with sides of equal length (equilateral) n should be equal to 3. w is a measure of cutout sharpness or softness. The conditions $0 \le w < 1/n$ ensure that the cutout shape does not have loops. Effect of the amount of w is shown in Fig. 1, according to this figure for a square cutout when w decreases, corners of the cutout become smoother until w reaches its minimum value, (becomes zero), in

this case, cutout converts to a circle. Fig. 2 shows the effect of w and n on the shape of polygonal cutout for zero rotation angle (β=0).The parameter β is the cutout orientation angle.

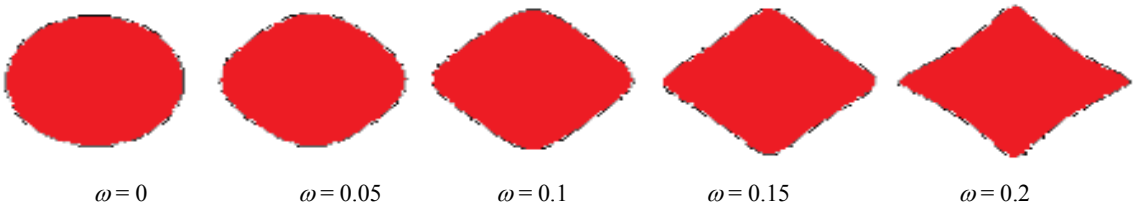

Fig.1
Effect of ω on the cutout geometry.

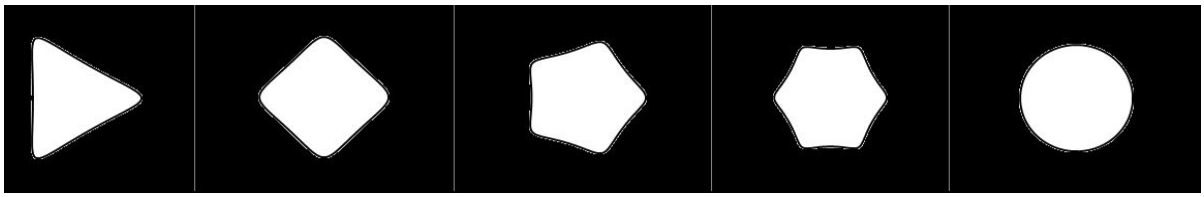

Fig.2
Effect of ω and n on the cutout shape.

Perforated FG plates considered in this study are exponential FG plate i.e. Young's modulus, Poisson's ratio and shear modulus of the point residing at the distance z relative to the total thickness are provided via the exponential function below:

$$M.P(z) = P_t e^{\eta(\frac{1}{2}+\frac{z}{H})} \tag{3}$$

Such that z is the gap from the X-Y plane at the plate center within the middle surface, $M.P(z)$ is the substance characteristic at distance z, $\eta = \ln\frac{P_b}{P_t}$, H is the total thickness, P_t is the substance characteristic in the top layer of the functionally graded plate and P_b the substance material in the bottom layer of the functionally graded plate. An illustrative presentation of the problem geometry is depicted in Fig. 3. For the considered laminate, top and bottom laminate have a 90-degree and 0-degree fiber angle, correspondingly.

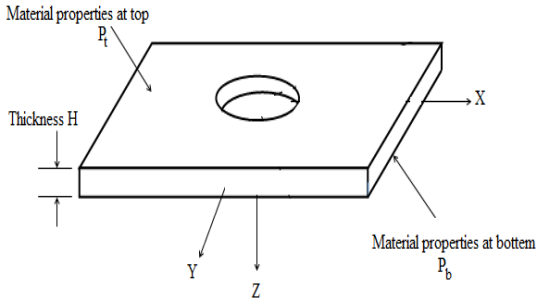

Fig.3
Functionally graded plate with a cutout (Dave and Sharma [17]).

The stress resultants and moments are obtained in terms of the stress function ϕ_j as relations (4) and (5) [3]:

$$N_x = 2\,\mathrm{Re}\sum_{j=1}^{4} s_j^2 \phi_j'(zp_j)$$
$$N_y = 2\,\mathrm{Re}\sum_{j=1}^{4} \phi_j'(zp_j) \tag{4}$$
$$N_{xy} = -2\,\mathrm{Re}\sum_{j=1}^{4} s_j \phi_j'(zp_j)$$

$$M_x = 2\,\mathrm{Re}\sum_{j=1}^{4} f_{1j}(s_j)\phi_j'(zp_j)$$
$$M_y = 2\,\mathrm{Re}\sum_{j=1}^{4} f_{2j}(s_j)\phi_j'(zp_j) \tag{5}$$
$$M_{xy} = 2\,\mathrm{Re}\sum_{j=1}^{4} f_{3j}(s_j)\phi_j'(zp_j)$$

In the above relations:

$$\begin{Bmatrix} f_{1j} \\ f_{2j} \\ f_{3j} \end{Bmatrix} = \begin{bmatrix} D_{11}^* & D_{12}^* & D_{16}^* \\ D_{12}^* & D_{22}^* & D_{26}^* \\ D_{16}^* & D_{26}^* & D_{66}^* \end{bmatrix} \begin{Bmatrix} -\mu_j(s_j) \\ -\mu_j(s_j)s_j^2 \\ -2\mu_j(s_j)s_j \end{Bmatrix} \tag{6}$$

which μ_j are the anisotropy factor. The stress functions ϕ_j may be computed using the superposition approach by aggregating the stress functions in two conditions. For the initial condition, a complete plate is assumed (excluding a cutout) under a load on outer edges. Such load creates an internal load on the points on the cutout limits. Regarding the main issue, the cutout boundary is not subjected to a load. For the second condition, it is assumed that an opposing force to the cutout boundary internal cutout offsets its impact. When there is no cutout, the stress function of the first condition may be clarified as a complex constant.

$$\phi_{1j}' = A_j \tag{7}$$

Due to the cutout boundary being considered to be free from traction, regarding the second condition, it is assumed that at the cutout boundary, an opposing force to the internal load stemming from the external load of the initial condition offsets its impact. Therefore, the boundary conditions are [17]:

$$2\,\mathrm{Re}\left[s_j \phi_{2j}(zp_j)\right] = 2\,\mathrm{Re}\left[s_j A_j zp_j\right] \tag{8}$$

$$2\,\mathrm{Re}\left[\phi_{2j}(zp_j)\right] = 2\,\mathrm{Re}\left[A_j zp_j\right] \tag{9}$$

$$2\,\mathrm{Re}\left[\frac{f_{1j}}{s_j}\phi_{2j}(zp_j)\right] = 2\,\mathrm{Re}\left[\frac{f_{1j}}{s_j}A_j zp_j\right] \tag{10}$$

$$2\,\mathrm{Re}\left[f_{2j}\phi_{2j}(zp_j)\right] = 2\,\mathrm{Re}\left[f_{2j}A_j zp_j\right] \tag{11}$$

Using the Schwartz formula concerning the holomorphic function ϕ_j and the substitution of the mapping function (1) in Eqs. (8) to (11) yields:

$$s_j\phi_{2j}(\zeta) = \frac{1}{2}\left[s_j A_j\left(a_j\zeta + \frac{b_j}{\zeta} + c_j\omega\zeta^n + \frac{d_j\omega}{\zeta^n}\right) + \bar{s}_j\bar{A}_j\left(\bar{a}_j\zeta + \frac{\bar{b}_j}{\zeta} + \bar{c}_j\omega\zeta^n + \frac{\bar{d}_j\omega}{\zeta^n}\right)\right] \tag{12}$$

$$\phi_{2j}(\zeta)=\frac{1}{2}\left[A_j(a_j\zeta+\frac{b_j}{\zeta}+c_j\omega\zeta^n+\frac{d_j\omega}{\zeta^n})+\bar{A}_j(\bar{a}_j\zeta+\frac{\bar{b}_j}{\zeta}+\bar{c}_j\omega\zeta^n+\frac{\bar{d}_j\omega}{\zeta^n})\right] \tag{13}$$

$$H_j\phi_{2j}(\zeta)=\frac{1}{2}\left[H_jA_j(a_j\zeta+\frac{b_j}{\zeta}+c_j\omega\zeta^n+\frac{d_j\omega}{\zeta^n})+\bar{H}_j\bar{A}_j(\bar{a}_j\zeta+\frac{\bar{b}_j}{\zeta}+\bar{c}_j\omega\zeta^n+\frac{\bar{d}_j\omega}{\zeta^n})\right] \tag{14}$$

$$f_{2j}\phi_{2j}(\zeta)=\frac{1}{2}\left[f_{2j}A_j(a_j\zeta+\frac{b_j}{\zeta}+c_j\omega\zeta^n+\frac{d_j\omega}{\zeta^n})+\bar{f}_{2j}\bar{A}_j(\bar{a}_j\zeta+\frac{\bar{b}_j}{\zeta}+\bar{c}_j\omega\zeta^n+\frac{\bar{d}_j\omega}{\zeta^n})\right] \tag{15}$$

where $H_j=\frac{f_{1j}}{s_j}$. Eqs. (12)-(15) are solved to determine ϕ'_{2j}. This gives the final solution for ϕ'_j as [20]:

$$\phi'_j(zp)=A_j-\frac{\phi'_{2j}(\zeta)}{zp'_j(\zeta)} \tag{16}$$

Such that zp' is the initial derivative of the mapping function in regard to ζ. Ultimately, by implementing Eq. (16) in Eqs. (4) and (5), the stress resultants and moments are acquired.

4 VALIDATION OF THE RESULTS

The outcomes of the provided analytical approach were assessed by the commercial FEM software. For this aim, cutout geometry was designed in ABAQUS by assuming β=0° (cutout orientation), c=1(aspect ratio of the cutout) and ω=0.125 (bluntness parameter). To simulate a functionally graded plate, it is assumed to be consisting of 100 layers with slightly varying properties, which make gradual changes of properties through the thickness. The applied load was set to $N_x=1N/mm$. To achieve the optimal mesh grid and improve the accuracy of the FEM results, the area around the cutout was modeled with a much smaller mesh than the farther areas. Meshing was performed by the use of S8R elements in accordance with the geometry and physics of the problem. To simulate a functionally graded plate, it is considered to include 100 layers with marginally differing characteristics that altogether create the eventual variances in characteristics along the thickness. The implemented load was $N_x=1N/mm$. For the purpose of obtaining an optimal mesh grid and enhancing the preciseness of FEM outcomes, the region at the cutout's proximity was modeled using a smaller mesh compared to farther regions. Meshing took place using S8R elements in regard to the physics and geometry of the issue at hand. Based on Fig. 4, the area at the vicinity of the cutout was examined with meshes in various sizes to approve the numerical solution and to ascertain the optimal quantity of meshes. In this area, the number of elements enhanced from 40 to 360 and it was evident upon such threshold increasing the number of elements does not significantly vary the outcomes. Therefore, this number of elements was considered as an optimal number of elements for the mesh and the results were obtained in this condition. The maximum stress resultants' ratio at the cutout corner to the implemented load is considered as the normalized stress resultant. Evidently, when the implemented load is 1 i.e. ($N_x=1N/mm$), hence the normalized stress resultant is the stress resultants. Furthermore, the normalized moment resultants (m_x, m_y and m_{xy}) are defined as ($\frac{M_x*1000}{\sqrt{Q_{11}N_xH}}$, $\frac{M_y*1000}{\sqrt{Q_{11}N_xH}}$, $\frac{M_{xy}*1000}{\sqrt{Q_{11}N_xH}}$) correspondingly, such that H is the overall laminate thickness [20]. The comparison of the normalized moment resultant m_x obtained from the analytical solution method and numerical solution for quasi-triangular cutout is shown in Fig. 5. Moreover, Fig. 6 provides a comparison of the stress resultant m_x acquired from the provided analytical solution including one provided by the numerical solution for FG plate with quasi-square cutout. The angle α denotes the points' position on the cutout boundary in regard to the horizontal axis. It can be seen that the results of two methods are close to each other and this confirms validity of the presented results. The mechanical characteristics considered for FGM are provided in Table 1.

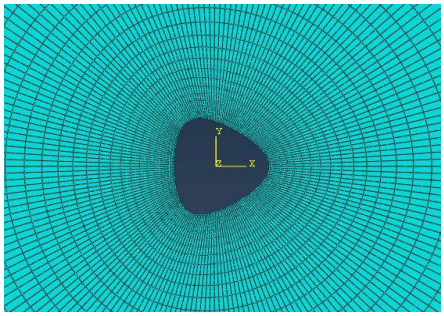

Fig.4
Mesh refinement for a plate with quasi-triangular cutout.

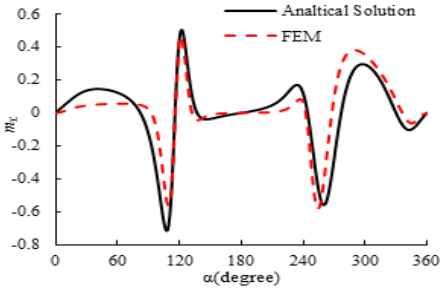

Fig.5
Comparing the stress resultant m_x for the quasi-triangular cutout in ω=0.125.

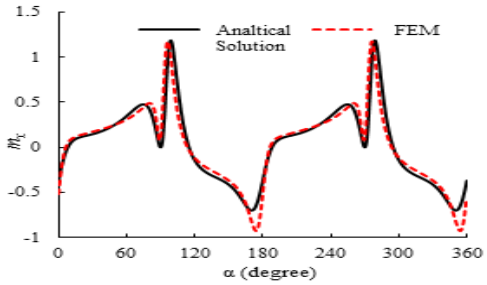

Fig.6
Comparing the stress resultant m_x for the quasi-square cutout in ω=0.125.

Table 1
Mechanical properties of the used material (Ashoori Savadkoohi and Jafari [20]).

Material	$E_1(GPa)$	$E_2(GPa)$	$G_{12}(GPa)$	ν_{12}
BMI	124	8.46	4.59	0.28

5 RESULTS AND DISCUSSIONS

In this section, the stress resultants and moments of functionally-graded plates with polygon cutout were investigated. The number of effective layers, rotation angle of cutout and bluntness parameter is the important parameters studied on triangular, square, pentagonal, and hexagonal cutouts in this paper.

5.1 Triangular cutout

In Fig. 7, the maximum stress resultants acquired around a triangular cutout in asymmetric laminate from modeling with 20 to 140 layers are presented. Evidently, as the number of the laminate (N) is increased, the stress resultant primarily increases and subsequently decreases until gradually reaching a constant value at N=90. Consequently, every research outcome was calculated with N=100 layer number, which is accordance to dimensionless ply thickness of 0.01.

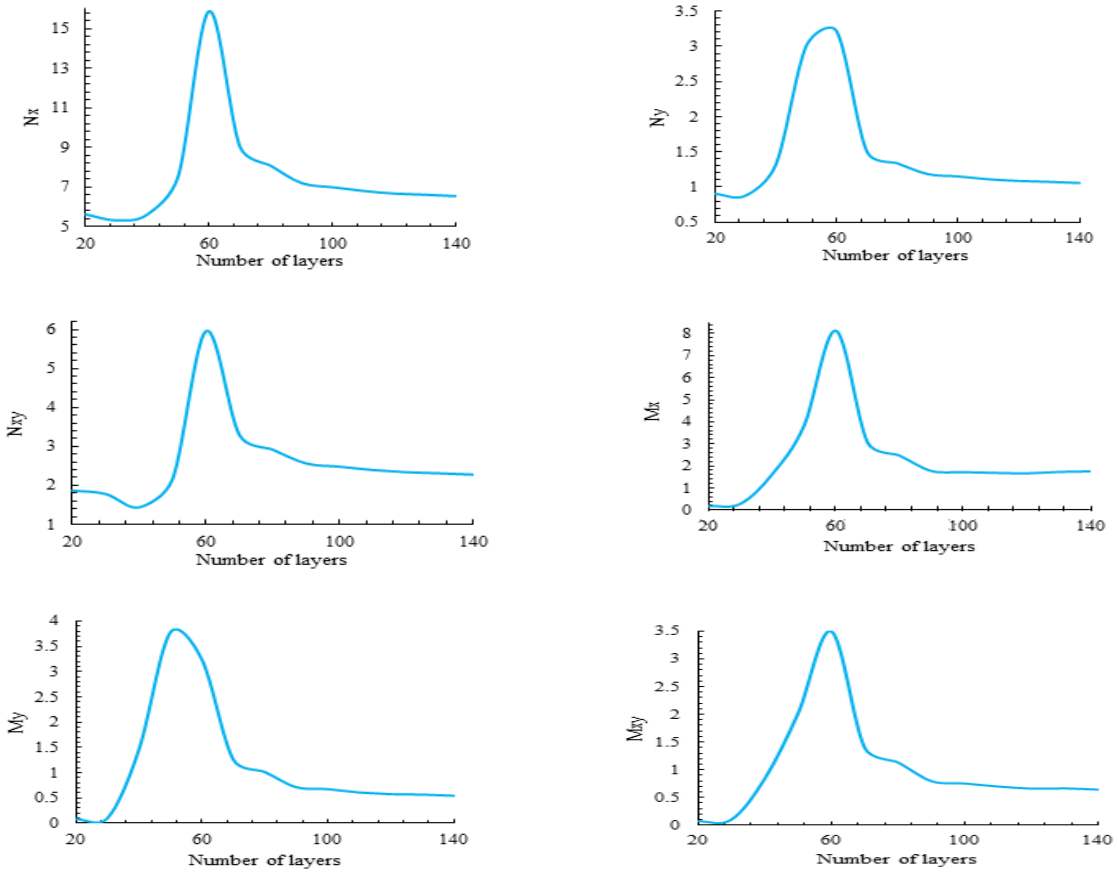

Fig.7
Stress resultants and moments for a various number of layers for triangular cutout.

Fig. 8 presents the discrepancies of the normalized stress resultants and moments with the rotation angle of the triangular cutout (β) in various values of bluntness parameter (ω). Because the difference of stress resultants with cutout orientation are periodical, the outcomes are provided for β values of up to 90 degrees. Based on this figure, for all values of ω, by decreasing the value of ω, the stress resultants and moments is reduced. In each value of ω, the minimum normalized stress resultants (n_x, n_y, n_{xy}) occur at approximately rotation angle of 45°. The rotation angle of 20° leads to the maximum normalized stress resultants. About moments, the minimum value of m_x happens at cutout orientation of 55°. The minimum values of m_y and m_{xy} occur at rotation angle of 20°. The variations of m_x and m_{xy} behave differently compared to m_x. The rotation angle of 50° leads to the maximum value of m_y and m_{xy}. In each figure, the minimum values of stress resultants and moments are called desirable stress resultants and moments and their maximum values are called undesirable stress resultants and moments. Table 2., presents the value of desirable and undesirable stress resultants and moments for the triangular cutout. Table 2., shows the importance of choosing the appropriate values of rotation angle in the analysis of FG plates with cutout.

Table 2
Desirable and undesirable resultants for triangular cutout with ω= 0.1.

Normalized stress resultants and moments	Desirable resultant	Rotation angle (degree)	Undesirable resultant	Rotation angle (degree)
n_x	5.33	50	6.4	20
n_y	0.71	45	0.91	15
n_{xy}	1.64	45	2.03	15
m_x	0.6	55	0.76	25
m_y	0.12	20	0.13	50
m_{xy}	0.11	20	0.13	50

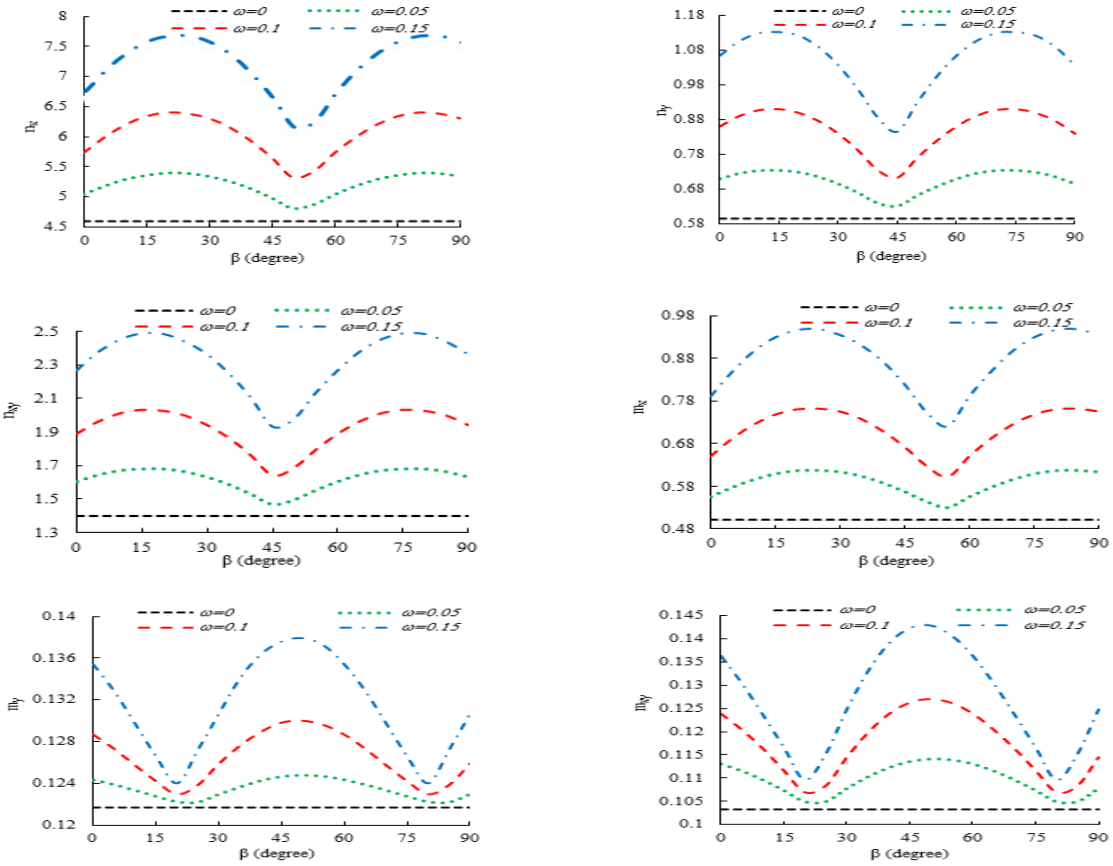

Fig.8
Variation of maximum stress resultants and moments with rotation angles (β) for triangular cutout.

The impact of c on the maximum stress resultants acquired with various curvature factors at zero-degree orientation (β=0) is shown in Fig. 9. Evidently, as c is increased, all resultants with the exception of m_{xy} enhanced linearly. This is evident in all values of bluntness parameter. As shown in Fig. 9, the lowest values of stress resultants and moments happen in ω=0 that is equal to a circular cutout. m_{xy} decreases by increasing the value of c.

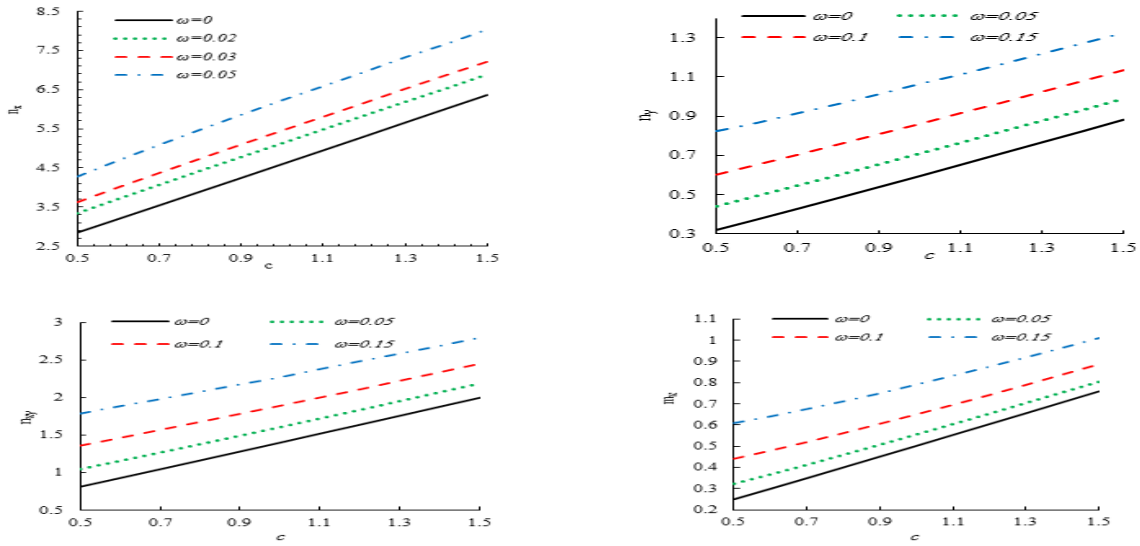

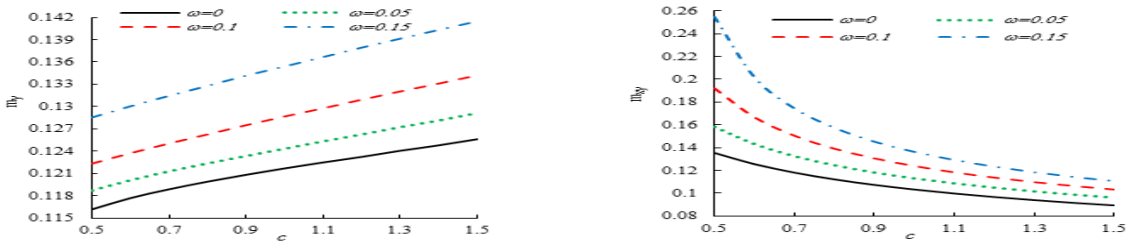

Fig.9
Effect of c on the stress resultants and moments in different values of ω for triangular cutout.

Fig. 10 depicts the impact of bluntness parameter (ω) on the normalized stress resultant at β=0 and c=1. In figure presents that as we increased ω to sharpen the cutout corners, the maximum stress resultants increased. The minimum amount of normalized stress resultants and moments occur at ω=0. As previously stated, ω= 0 is the equivalent of a circular cutout. As illustrated in this figure, the rotation angle of 45° compared to two other angles leads to the minimum values of normalized stress resultants. The maximum values of n_x and n_{xy} occur at a rotation angle of 30° however, for n_y this value occurs at a rotation angle of zero degree. The rotation angle of 30° causes the minimum values of m_y and m_{xy}, however, the minimum value of m_x occurs at a rotation angle of zero degree.

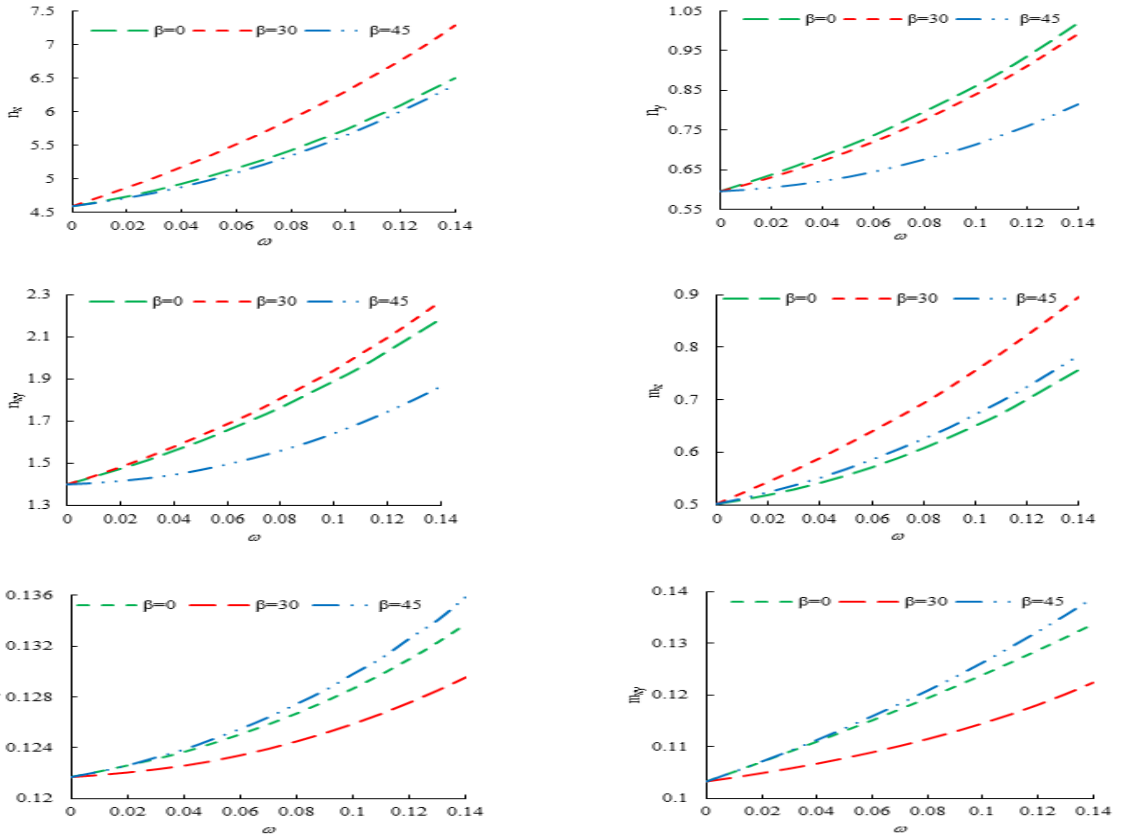

Fig.10
The effect of ω on the normalized stress resultants and moments for triangular cutout.

5.2 Square cutout

This section presents an attempt to study to the impact of vital factors such as the cutout orientation, the bluntness factors and aspect ratio of the cutout on stress distribution at the vicinity of a quasi-square cutout in FG plate. Fig. 11 presents the differences in normalized stress resultants and moments at various cutout orientations (β) at various bluntness parameter values (ω). Due to the sporadic activity of the stress resultant with cutout orientation, the

outcomes are shown for β values of up to 90°. Based on this figure, in a number of cutout orientation, the stress resultant n_x acquired at nonzero ω values (i.e. non-circular cutout) are less compared to the n_x acquired at ω=0 (i.e. circular cutout). At lower values ofω, the broader is the extent of β values where such occurrence is seen. The least value of stress resultant n_x is acquired at ω=0.1 with β of approximately 30 degrees. Regarding n_y, the least value is seen at a rotation angle of 22.5°, and ω=0.05 for other values of ω, the least values of n_y are seen at a rotation angle of approximately 20°. For a broad extent of β values, the stress resultant acquired with ω=0.05 is less compared to the value acquired at ω=0. The differences of n_{xy} with cutout orientation (β) are almost identical to those of n_x. Concerning every value of the bluntness factor, the least n_{xy} was seen at the rotation angle of approximately 30 degrees. Also, the lowest value of moment resultant m_x is obtained at ω=0.1 and rotation angle of about 45 degrees. Also, the lowest values of moments m_y and m_{xy} are obtained at ω=0.15 and ω=0.05 with β of about 10° and 45°, respectively. Table 3., presents the values of desirable and undesirable normalized stress resultants and moments for the square cutout in FG plate.

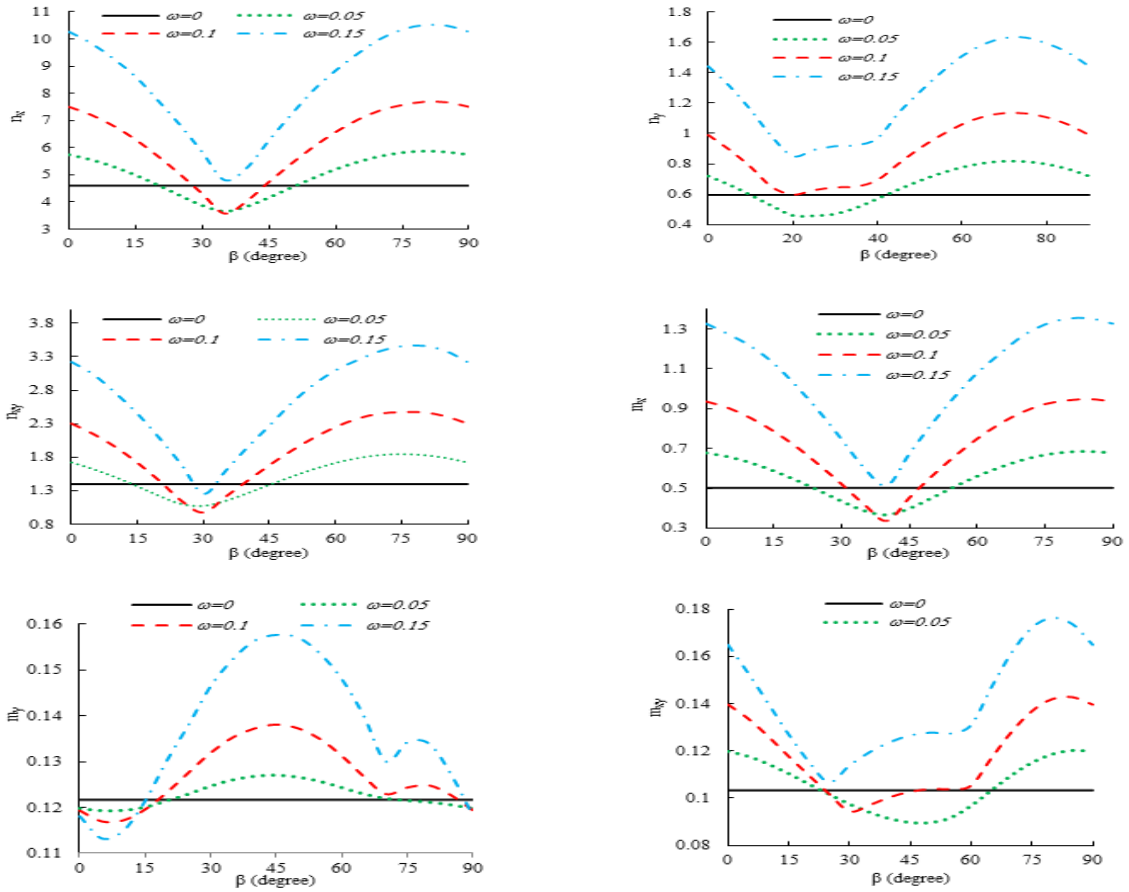

Fig.11
Variation of stress resultants and moments with different cutout orientation for square cutout.

Table 3
Desirable and undesirable resultants for square cutout with ω= 0.05.

Normalized stress resultants and moments	Desirable resultant	Rotation angle (degree)	Undesirable resultant	Rotation angle (degree)	Cirular resultant
n_x	3.65	35	5.87	80	4.6
n_y	0.46	25	0.82	70	0.6
n_{xy}	1.07	30	1.85	75	1.4
m_x	0.37	40	0.69	85	0.5
m_y	0.12	10	0.13	45	0.12
m_{xy}	0.09	50	0.12	85	0.10

The impact of the cutout aspect ratio on maximum stress resultants and moments with various ω values at zero-degree rotation angle (β=0) is depicted by Fig. 12. It is evident that by enhancing the value of c, every stress resultant is enhanced linearly. But for the moment resultants, this behavior is not seen. For example for ω=0.15, from c=0.5 to c=0.6, the normalized moment m_x decreases then increases similar to other investigated values of bluntness parameter. Moreover, for the normalized moment m_y, a completely different behavior can be observed. m_{xy} decreases by increasing the value of c.

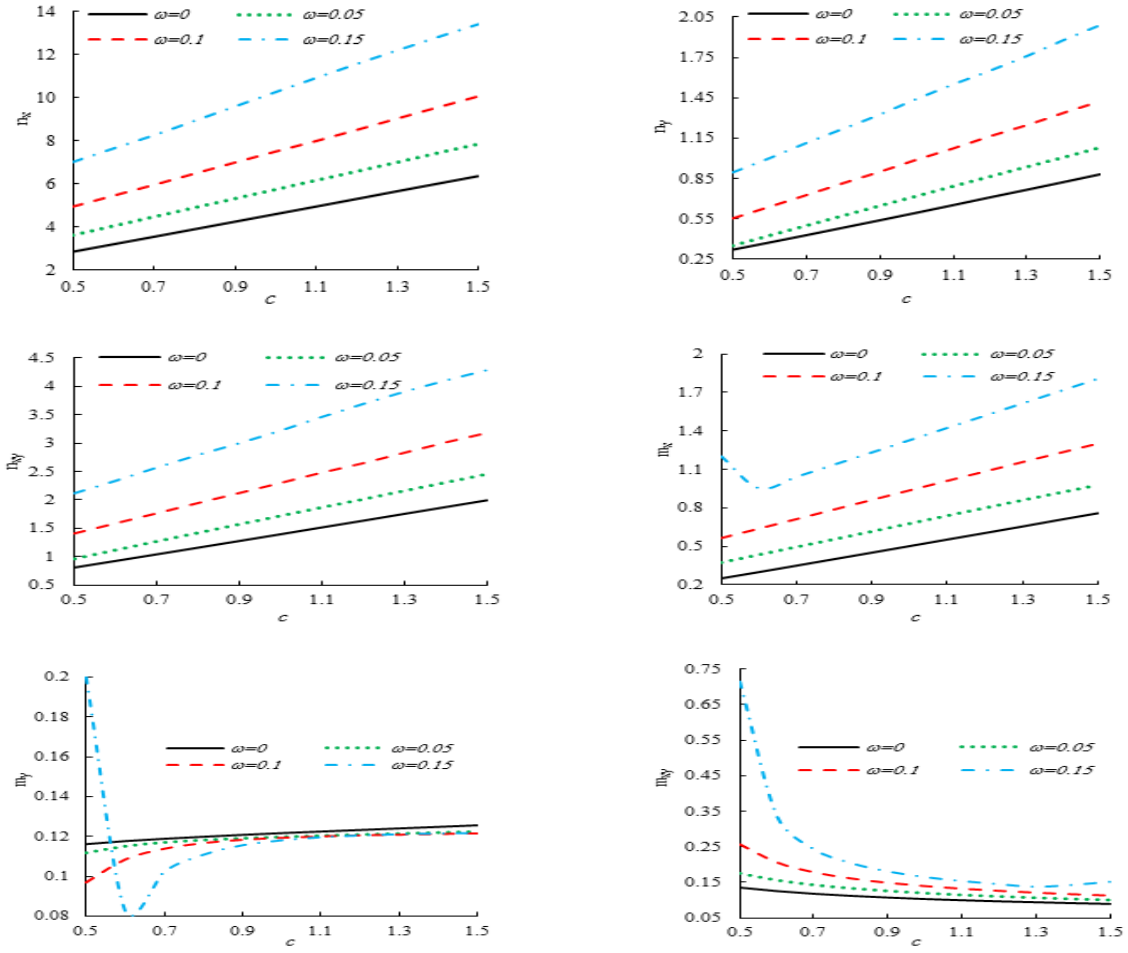

Fig.12
Effect of c on the stress resultants and moments in different values of ω for square cutout.

Fig. 13 shows the impact of the normalized stress resultants and moments' bluntness factor at the vicinity of the quasi-square cutout (c=1) for a rotation angle of 0°. According to this figure, the least value of normalized stress resultants and moments take place at $\omega \neq 0$. Thus, the circular cutout is not in ideal shape for FG plates' cutout. The maximum normalized stress resultants and moments that are less compared to the circular cutout may be realized by choosing the suitable rotation angle values. As illustrated in this figure, the rotation angle of 30° for the normalized stress resultants and 45° for the normalized moments compared to two other angles leads to the minimum values of normalized stress resultants and moments. The maximum values of n_x and n_{xy} occur at a rotation angle of zero, however, for n_y this value occurs at a rotation angle of 60° degrees. Furthermore, the maximum values of m_x and m_{xy} occur at a rotation angle of zero however, for this value occurs at a rotation angle of 45° degrees.

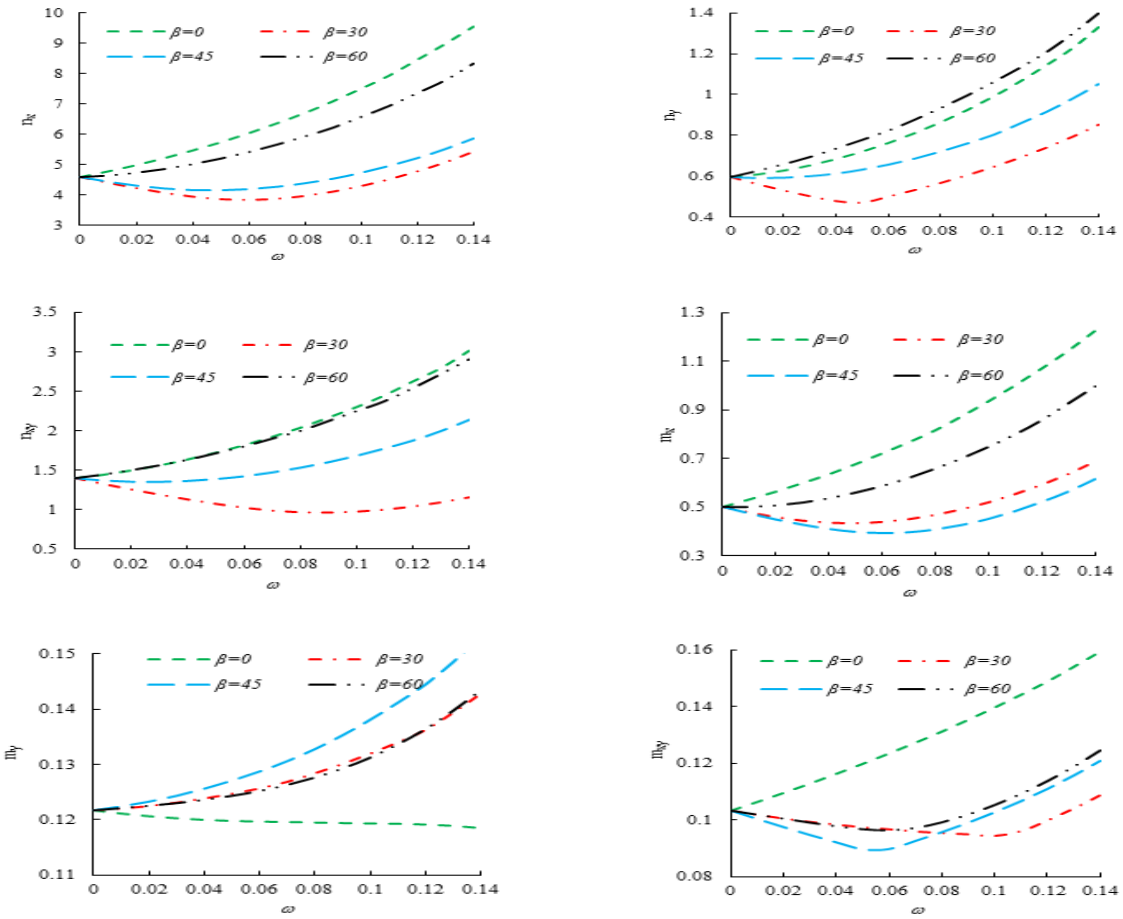

Fig.13
Effect of ω on the normalized stress resultant and moments for square cutout.

5.3 Pentagonal cutout

The impact of vital factors such as the aspect ratio of the cutout, the cutout orientation and bluntness factors on the distribution at the vicinity of the pentagonal cutout within the FG plate is examined here. Fig. 14 depicts the differences in normalized stress resultants and moments interms of rotation angle of the pentagonal cutout (β) in various values of bluntness parameter (ω). Due to the periodic nature of the stress resultants with cutout orientation, the outcomes are shown for β values of up to 36 degrees. According to this figure, for all values of ω, by raising the quantity of ω, the value of stress resultants and moments is increased. In each value of ω, the minimum normalized stress resultants (n_x , n_y , n_{xy}) occur at approximately rotation angle of 26°, 15° and 20°, respectively. Furthermore, the minimum normalized moment resultants (m_x , m_y , m_{xy}) occur at approximately rotation angle of 30°, 24° and 21°, respectively. Table 4 presents the value of desirable and undesirable normalized stress resultants and moments for the pentagonal cutout.

Table 4
Desirable and undesirable resultants for pentagonal cutout with ω= 0.03.

Normalized stress resultants and moments	Desirable resultant	Rotation angle (degree)	Undesirable resultant	Rotation angle (degree)
n_x	5.07	27	5.58	9
n_y	0.68	15	0.77	0
n_{xy}	1.56	21	1.74	3
m_x	0.56	30	0.64	12
m_y	0.12	24	0.13	6
m_{xy}	0.11	21	0.12	0

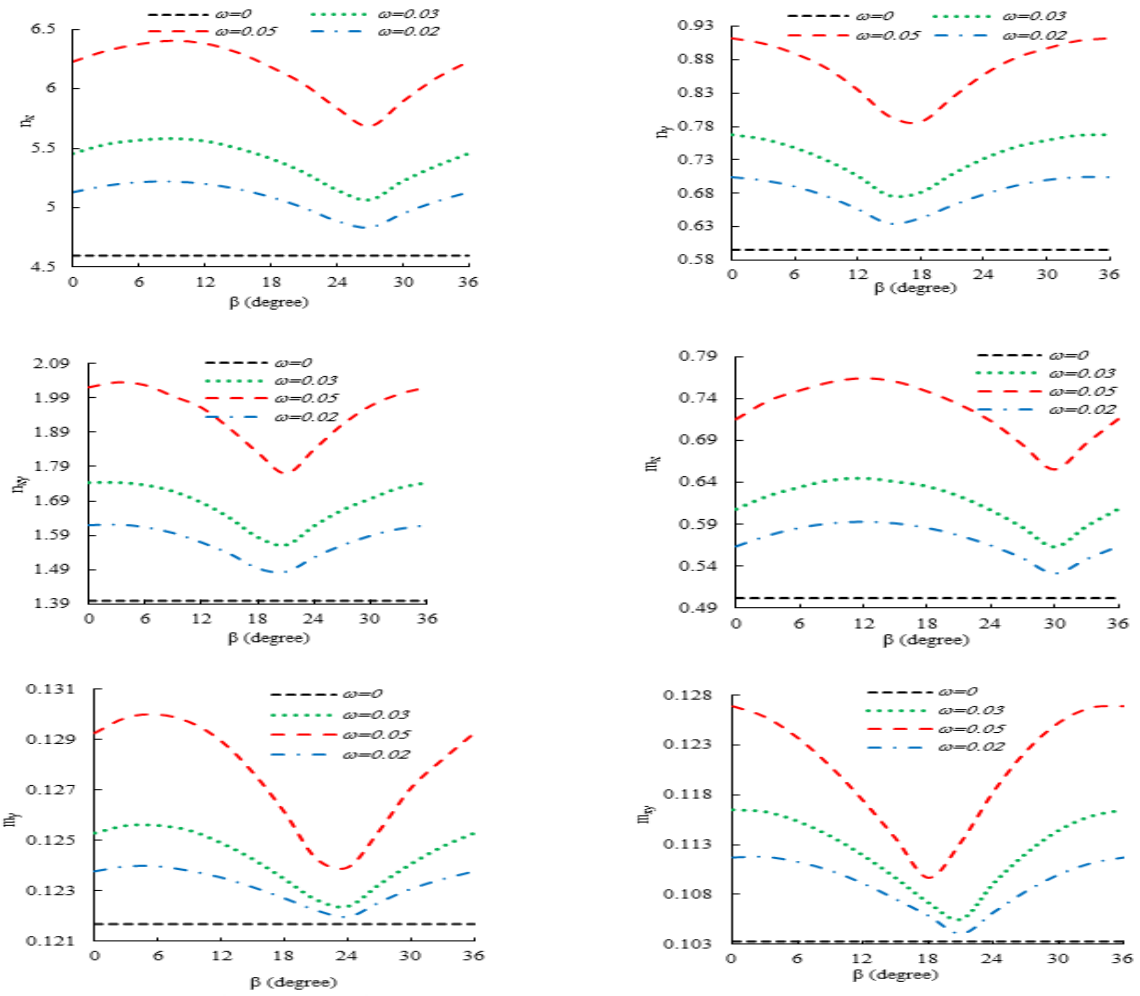

Fig.14
Variation of normalized stress resultants and moments with orientation angles for pentagonal cutout.

The aspect ratio of the cutout is one of the important parameters in stress analysis of perforated FG plate. The impact of this factor on normalized stress resultants and moments in different values of bluntness factor and zero degree orientation cutouts are shown in Fig. 15. As observed, with increasing c, all stress resultants increase linearly. This is observed for all values of bluntness parameter. As shown in this figure, the lowest values of stress resultants and moments happen in ω=0 which is equivalent to a circular cutout. m_{xy} decreases by increasing the value of c.

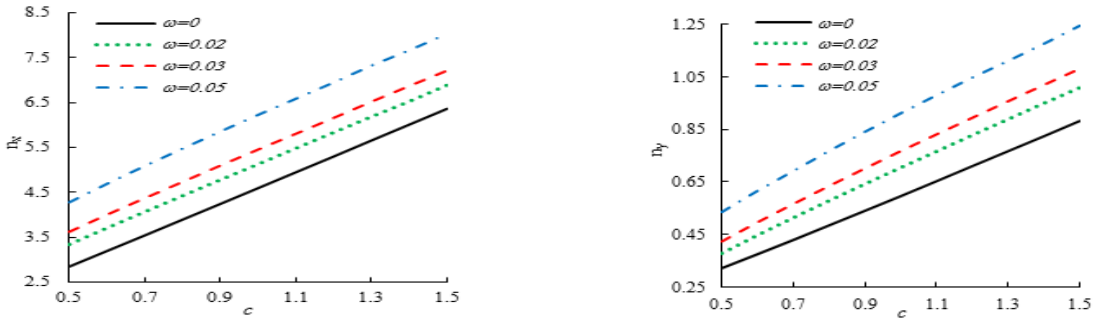

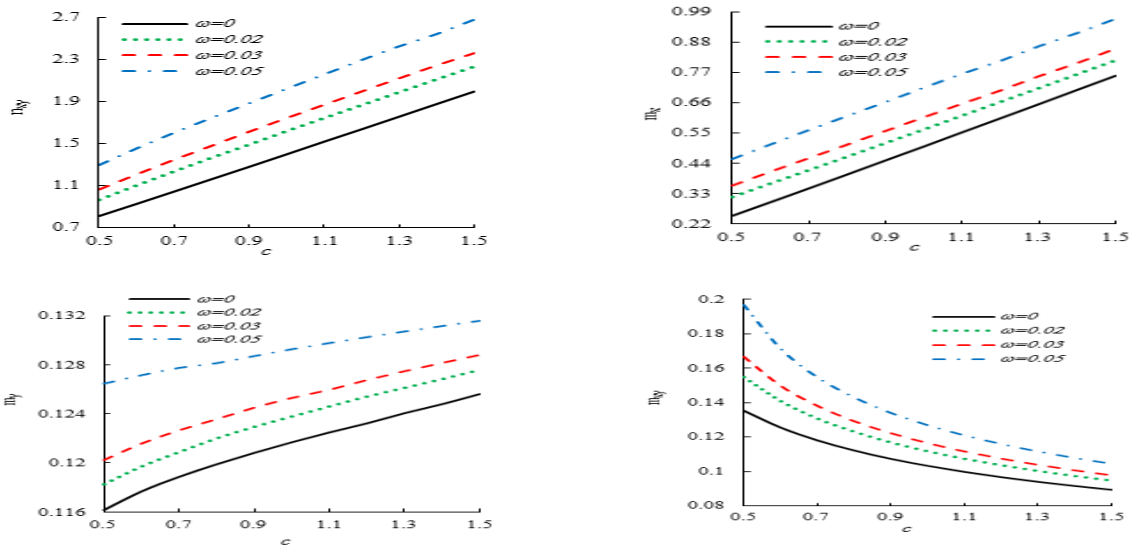

Fig.15
Effect of c on the stress resultants and moments in different values of ω for pentagonal cutout.

For rotation angle of 0° and c=1, Fig. 16 shows the efficacy of bluntness parameter on the normalized stress resultants and moments. This figure illustrates that as we increased ω to sharpen the cutout corners, the normalized stress resultants increased. The minimum value of normalized stress resultants and moments occur at ω=0. As previously stated, ω= 0 is the equivalent of a circular cutout. As shown in this figure, the minimum values of n_x and n_{xy} occur at a rotation angle of 30° however, for n_y this value occurs at a rotation angle of 45° Whereas, maximum values of m_x and m_y occur at a rotation angle of 45° and for m_{xy} this value occurs at a rotation angle of 30 degrees.

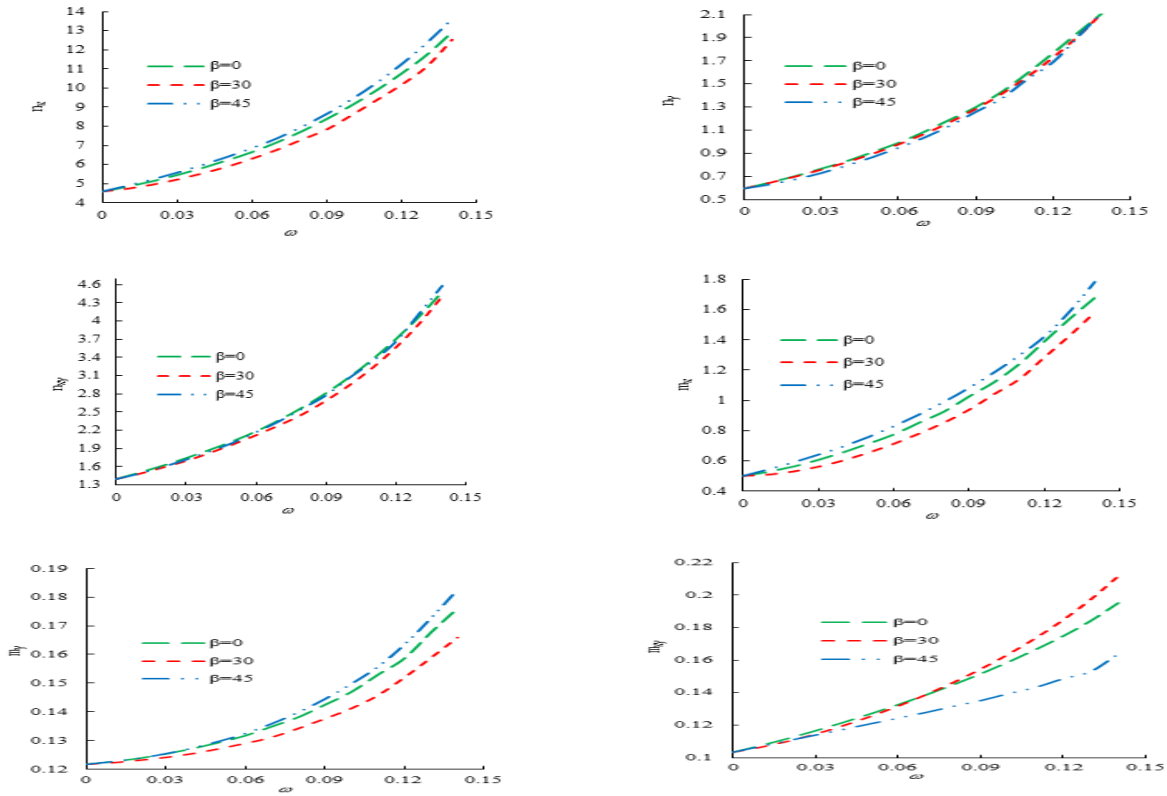

Fig.16
Effect of ω on the normalized stress resultants and moments for pentagonal cutout.

5.4 Hexagonal cutout

The changes in normalized stress resultants and moments with cutout orientation for FG plate including hexagonal cutout is depicted in Fig. 17 for various ω values. Since the stress resultants variation with orientation angle is of a sporadic nature, the outcomes are shown for β values of up to 60°. It is evident from this figure that regarding various cutout orientation angles, the stress resultants n_x, n_y and n_{xy} acquired at $\omega \neq 0$ (i.e. non-circular cutout) are less than acquired at ω=0 (circular cutout). The lowest value of stress resultants n_x, n_y and n_{xy} is achieved at ω=0.03 with β of about 45°. Moreover, for the moments m_x, m_y and m_{xy} , the lowest values are achieved at nonzero bluntness factor ($\omega \neq 0$). The lowest value of moment resultant m_x and m_{xy} was obtained at ω=0.03 with β of about 50 degrees. Also, the lowest value of moment resultant was obtained at ω=0.05 with β of about 10 degrees. Table 5., presents the value of the desirable and undesirable stress resultants and moments for the hexagonal cutout. Table 5., shows the importance of choosing the appropriate values of rotation angle in the analysis of plates with cutout.

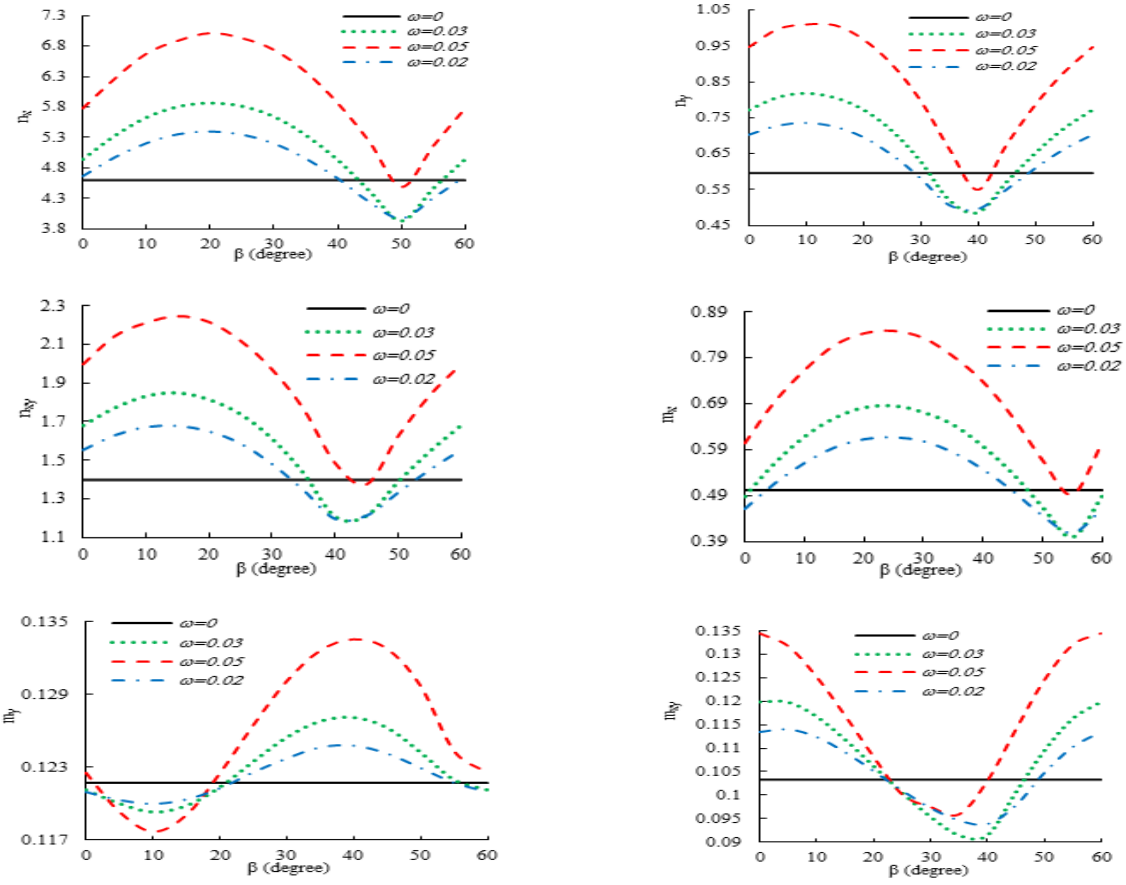

Fig.17
Variation of maximum stress resultants and moments with cutout orientation for hexagonal cutout.

Table 5
Desirable and undesirable resultants for hexagonal cutout with ω= 0.05.

Normalized stress resultants and moments	Desirable resultant	Rotation angle (degree)	Undesirable resultant	Rotation angle (degree)	Cirular resultant
n_x	3.97	50	5.40	20	4.6
n_y	0.50	40	0.74	10	0.6
n_{xy}	1.20	40	1.68	15	1.4
m_x	0.41	55	0.62	25	0.5
m_y	0.12	10	0.12	40	0.12
m_{xy}	0.09	40	0.11	5	0.10

The changes in normalized stress resultants and moments with an aspect ratio of the hexagonal cutout at various bluntness factor values and at zero degree orientation (β=0) is shown in Fig. 18. As shown in this figure, except for m_{xy}, the rest of the stress resultants and moments increase with increasing ω. For all the resultants except m_{xy}, the resultants with the bluntness parameter changes linearly. This is observed almost for all values of bluntness parameter.

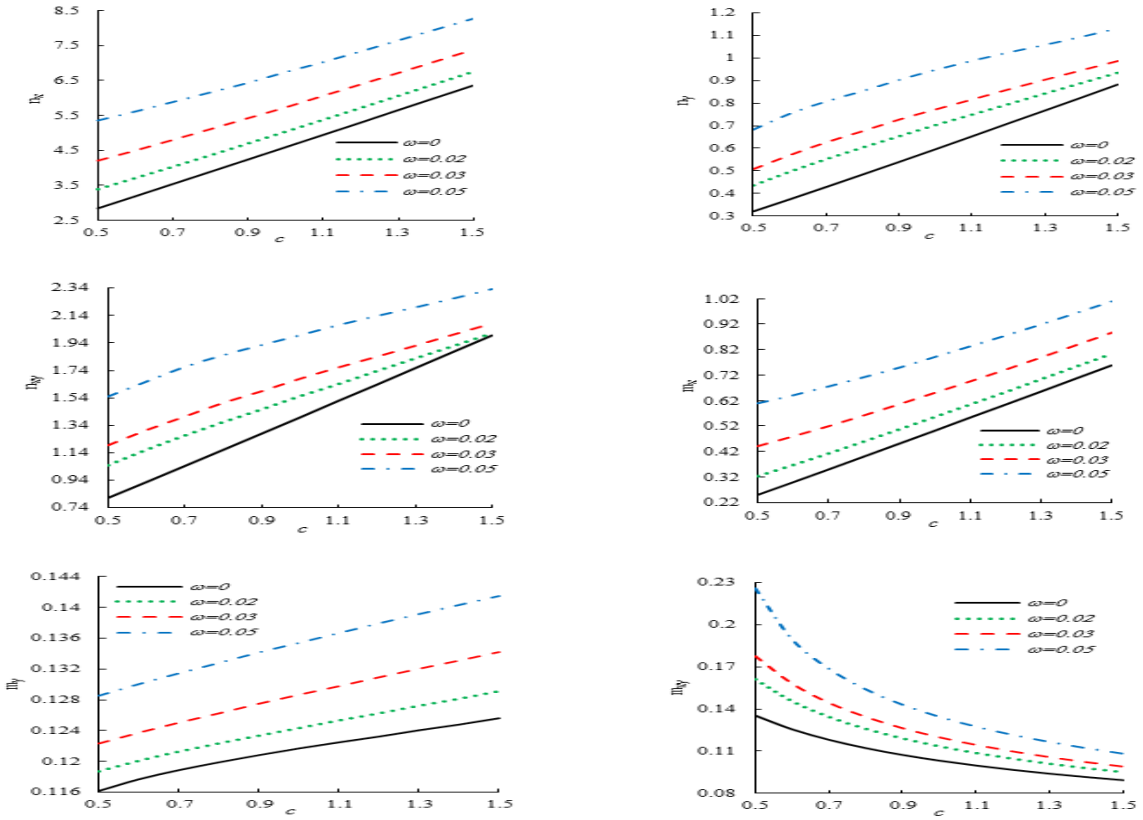

Fig.18
Effect of c on the stress resultants and moments in different values of ω for hexagonal cutout.

In various rotation angle values of the hexagonal cutout and for c=1, Fig. 19 shows the effect of bluntness parameter (ω) on the normalized stress resultants and moments. This figure shows that the minimum value of normalized stress resultants and moments occur at $\omega \neq 0$ depicts the impact of the bluntness factor (ω) on the normalized stress resultant and moments. As evident in this figure, the least value for normalized stress resultants and moments take place at $\omega \neq 0$. Thus, the circular cutout is not ideal for the cutout in FG plates. The normalized stress resultants and moments less than circular cutout may be realized by choosing the suitable rotation angle values. As depicted in this figure, a 45° rotation angle for normalized stress resultants entails minimum normalized stress resultant values. This rotation angle to achieve the minimum normalized moments is zero degrees.

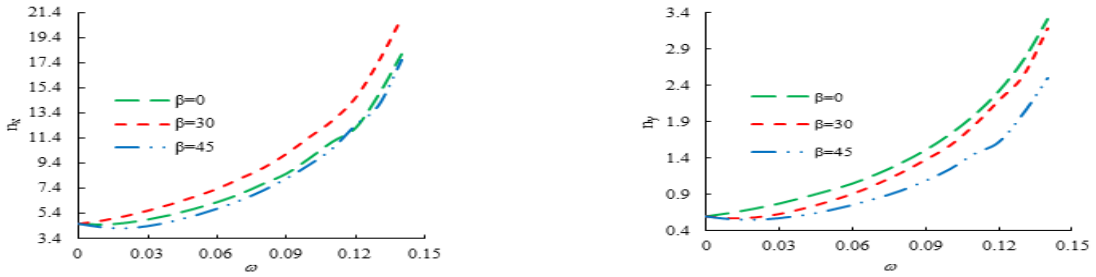

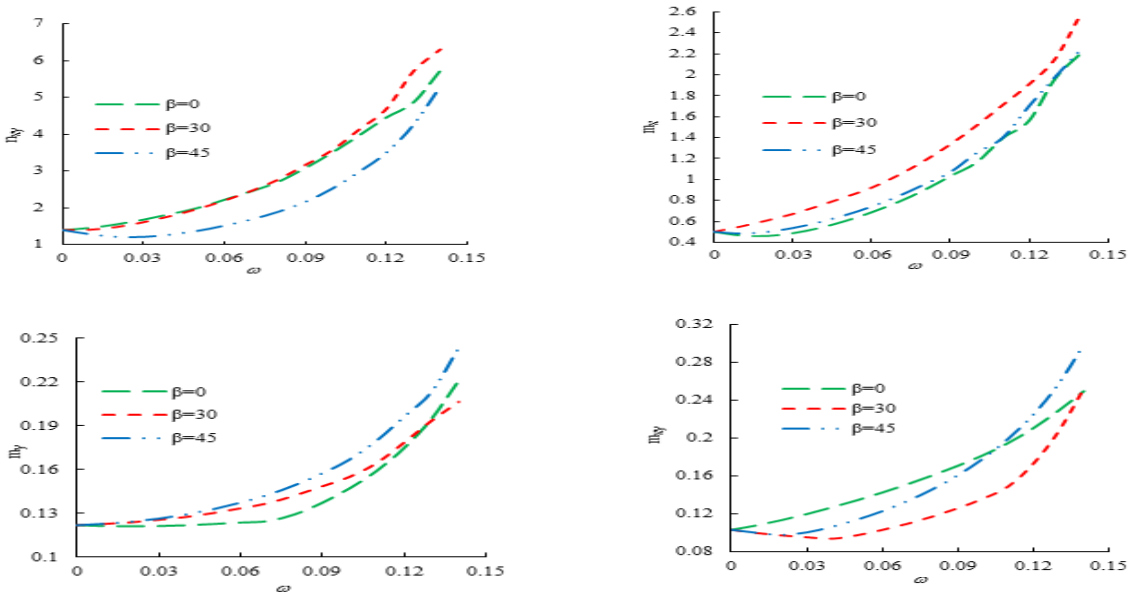

Fig.19
Effect of ω on the normalized stress resultant and moments for hexagonal cutout.

6 CONCLUSIONS

This paper presented an analytic method based on Lekhnitskii's complex-variable method and a mapping function for examining the stress distribution of functionally-graded plates with polygonal cutouts. The shape of the cutout and many parameters affect the location and value of the maximum stress. In this study, the effect of various parameters on stress distributions around different cutouts in an infinite FGM plate was separately investigated. The results showed that:

- The values of the maximum stress and moment resultants for all cutouts with an odd number of sides were always more than the corresponding value of a circular cutout while, all cutouts with an even number of sides were more efficient than circular cutout.
- Among of all cutout shapes, quasi-square cut-out has the lowest possible maximum stress and moment resultants. Hence, carefully adjustment of these parameters can significantly reduce the stress and moment resultants for all cutouts with any given corner curvature.
- The results obtained with some non-circular cutouts may even surpass the results normally given by cutouts of circular cross-section.
- Comparison of the presented analytical solution with the numerical solution obtained by finite element modeling demonstrated good consistency between these results.

REFERENCES

[1] Muskhelishvili N.,1954, *Some Basic Problems of the Mathematical Theory of Elasticity*, Dordrecht, Springer, Netherlands.
[2] Savin G.N.,1961, *Stress Concentration Around Holes*, Pregamon Press.
[3] Lekhnitskiy S.G.,1969, *Anperforated Plates*, New York, Gordon-Breach Science.
[4] Sharma D. S., 2012, Stress distribution around polygonal cutouts, *International Journal of Mechanical Sciences* **65**(1): 115-124.
[5] Sharma D.S., 2014, Moment distribution around polygonal cutouts in infinite plate, *International Journal of Mechanical Sciences* **78**: 177-182.
[6] Rezaeepazhand J., Jafari M.,2010, Stress concentration in metallic plates with special shaped cutout, *International Journal of Mechanical Sciences* **52**(1): 96-102.
[7] Ukadgaonker V.G., Rao D.K.N., 2000, A general solution for stress resultants and moments around cutouts in unsymmetric laminates, *Composite Structures* **49**(1): 27-39.

[8] Bayati Chaleshtari M.H., Jafari M., 2017, Optimization of finite plates with polygonal cutout under in-plane loading by gray wolf optimizer, *The Journal of Strain Analysis for Engineering Design* **52**(6): 365-379.
[9] Jafari M., Bayati Chaleshtari M.H., 2017, Optimum design of effective parameters for orthotropic plates with polygonal cut-out, *Latin American Journal of Solid and Structure* **14**(5): 906-929.
[10] Jafari M., Moussavian H., Bayati Chaleshtari M.H., 2018, Optimum design of perforated orthotropic and laminated composite plates under in-plane loading by genetic algorithm, *Structural and Multidisciplinary Optimization* **57**(1): 341-357.
[11] Yang Q., Gao C.-F., Chen W., 2012, Stress concentration in a finite functionally graded material plate, *Science China Physics, Mechanics and Astronomy* **55**(7): 1263-1271.
[12] Sharma D.S., 2011, Stress concentration around circular / elliptical / triangular cutouts in infinite composite plate, *Proceedings of the World Congress on Engineering*.
[13] Pan E., 2003, Exact solution for functionally graded anisotropic elastic composite laminates, *Journal of Composite Materials* **37**(21): 1903-1920.
[14] Reid R., Paskaramoorthy R., 2011, An extension to classical lamination theory for use with functionally graded plates, *Composite Structures* **93**(2): 639-648.
[15] Uymaz B., Aydogdu M., 2013, Three dimensional mechanical buckling of FG plates with general boundary conditions, *Composite Structures* **96**:174-193.
[16] Batra R.C., Nie G.J., 2010, A analytical solutions for functionally graded incompressible eccentric and non-axisymmetrically loaded circular cylinders, *Composite Structures* **92**(5): 1229-1245.
[17] Dave J.M., Sharma D.S., 2016, Stresses and moments in through-thickness functionally graded plate weakened by circular/elliptical cut-out, *International Journal of Mechanical Sciences* **105**: 146-157.
[18] Chien R.D., Lin C.Y., Chen C.S., 2011, Thermally induced buckling of functionally graded hybrid composite plates, *International Journal of Mechanical Sciences* **53**: 51-58.
[19] Joshi P.V., Gupta A., Jain N.K., Salhotra R., Rawani A.M., Ramtekkar G.D., 2017, Effect of thermal environment on free vibration and buckling of partially cracked isotropic and FGM micro plates based on a non classical Kirchhoff's plate theory: An analytical approach, *International Journal of Mechanical Sciences* **132**: 155-170.
[20] Jafari M., Ashoori H.S., 2015, Studying the effect of different parameters on stress resultant and moments distribution around non-circular cutouts in unsymmetric laminates, *ZAMM - Journal of Applied Mathematics and Mechanics* **97**(10): 1317-1330.
[21] Jafari M., Bayati Chaleshtari M.H., Ardalani E., 2018, Determination of optimal parameters for finite plates with a quasi-square hole , *Journal of Solid Mechanics* **10**(2): 300-314.
[22] Bayati Chaleshtari M.H., Jafari M., 2017, Using dragonfly algorithm for optimization of orthotropic infinite plates with a quasi-triangular cut-out, *European Journal of Mechanics A/Solids* **66**(1): 1-14.
[23] Nirwal S., Sahu S.A., Baroi J., Singh A., 2019, Analysis of different boundary types on wave velocity in bedded piezo-structure with flexoelectric effect, *Composites Part B: Engineering* **167**: 434-447.
[24] Sahu S.A., Singhal A., Chaudhary S., 2017, Surface wave propagation in functionally graded piezoelectric material: An analytical solution, *Journal of Intelligent Material Systems and Structures* **29**(3): 423-437.
[25] Singhal A., Sahu S.A., Chaudhary S., 2018, Approximation of surface wave frequencyin piezo-composite structure, *Composites Part B: Engineering* **144**: 19-28.
[26] Singhal A., Sahu S.A., Chaudhary S., 2017, Liouville-green approximation: an analytical approach to study the elastic waves vibrations in composite structure of piezo material, *Composite Structures* **184**: 714-727.
[27] Chaudhary S., Sahu S.A., Singhal A., 2017, Analytic model for Rayleigh wave propagation in piezoelectric layer overlaid orthotropic substratum, *Acta Mechanica* **228**(2): 495-529.
[28] Singh M.K., Sahu S.A., Singhal A., Chaudhary S., 2018, Approximation of surface wave velocity in smart composite structure using Wentzel–Kramers–Brillouin method, *Journal of Intelligent Material Systems and Structures* **29**(18): 3582-3597.
[29] Chaudhary S., Sahu S.A., Dewangan N., Singhal A., 2018, Stresses produced due to moving load in a prestressed piezoelectric substrate, *Mechanics of Advanced Materials and Structures* **26**(12): 1028-1041.
[30] Chaudhary S., Sahu S.A., Singhal A., 2018, On secular equation of SH waves propagating in pre-stressed and rotating piezo-composite structure with imperfect interface, *Journal of Intelligent Material Systems and Structures* **29**(10): 2223-2235.